16th World Conference on Earthquake, 16WCEE 2017

Santiago Chile, January 9th to 13th 2017

Paper N° 3907 (Abstract ID)

Registration Code: S-A1463116311

THE EFFECTS OF SUBSURFACE STRUCTURE ON DAMAGE CONCENTRATION IN A MOUNTAINOUS AREA

M. Koie(1), T. Maeda(2)

(1) *Graduate student, Dept. of Architecture, Waseda University, Tokyo, Japan, w.mk1919@moegi.waseda.jp*
(2) *Professor, Dept. of Architecture, Waseda University, Dr. Eng. Tokyo, Japan, tmaeda@waseda.jp*
…

Abstract

The 2014 Nagano prefecture Kamishiro fault Earthquake of magnitude 6.7 occurred on November 22, which jolted central mountainous area in Japan. The maximum seismic intensity was lower 6 on the Japanese scale of 7. Fortunately there was no dead or missing, but a lot of houses were damaged in northern part of Nagano prefecture, including Hakuba village. According to the local government statistics, damaged houses in the village were remarkably concentrated in two areas namely Horinouchi and Mikkaichiba. There found 39 houses collapsed and 51 houses partially destroyed, while damaged houses were scarcely observed in the surrounding areas of several km expanse. On the cause of the damage concentration in the village, general conclusions have not been reached so far.

Our study is aiming at contribution of shallow subsurface structure to the local damage concentration. We carried out high density micro-tremor observation in the area at sixty locations using portable miniature array of radius 0.9 m in the summer of 2015. K-NET and KiK-net earthquake observation stations, which are outside of damage concentrated area, were included since they are with PS logging data. We extracted dispersion curves and H/V spectra from the micro-tremor observation, deduced average shear wave velocity from Rayleigh wave velocity at reference wavelengths, and inferred surface layer thickness from predominant frequency of H/V spectra by the law of quarter wavelength. We conclude that the areas with thick soft layer encircled by relatively hard soil were seriously damaged.

Keywords: Kamishiro Fault Earthquake, Dispersion curves, Micro-tremor array observation, H/V spectra

1. Introduction

The 2014 Nagano prefecture Kamishiro fault Earthquake of magnitude 6.7 occurred on November 22, which jolted central mountainous area in Japan. The maximum seismic intensity was lower 6 on the Japanese scale of 7. Fortunately there was no dead or missing, but a lot of houses were damaged in northern part of Nagano prefecture, including Hakuba village. According to the local government statistics, the damaged houses were remarkably concentrated in two areas namely Horinouchi and Mikkaichiba. There found 39 houses collapsed and 51 houses partially destroyed, while damaged houses were scarcely observed in the surrounding areas of several km expanse. [1].

Variability of ground motion in the village was observed in aftershocks [1]. Seismic intensity for aftershocks in Horinouchi was larger than the outside reference point by 1 due to the amplification between 0.5 s and1.0 s periods. A soft subsurface layer of about 30 m thick was evaluated at some locations in Horinouchi by micro-tremor array observation with array radii between 1.5m and 20m. The soft layer can be partly attributable to the amplification, but the amplification level is not large enough to explain the damage. There are several studies on the cause of the damage concentration in the village; however, general conclusions have not been reached so far. Deep soil configuration might be necessary to explain the gap [1].

Our study is aiming at contribution of shallow subsurface structure to the damage concentration. We carried out high density micro-tremor observation in the area at sixty locations using portable miniature array of radius 0.9 m in the summer of 2015. K-NET and KiK-net earthquake observation stations, which are outside of damage concentrated area, were included since they are with PS logging data. We extracted dispersion curves and H/V spectra from the micro-tremor observation, deduced average shear wave velocity from Rayleigh wave velocity at reference wavelength, and inferred surface layer thickness from predominant frequency of H/V spectra by the law of quarter wavelength. We conclude that the areas with thick soft layer encircled by relatively hard soil were seriously damaged.

2. Micro-tremor observation and analysis

Fig.1 shows the locations where we took pictures in our preliminary survey two weeks after the earthquake. The distribution of photo spots implies the distribution of damaged houses. Micro-tremor observation points were arranged following the distribution of damaged houses; 14 points in Horinouchi, 8 points in Mikkaichiba, 15 points in Tagashira shown in Fig. 2. These areas will be hereafter referred as Kamishiro area.

Array configuration is shown in Fig. 3. Six servo accelerometers were used, three of them were placed in the array center and others were placed at the periphery of a circle of 0.9 m radius to make a regular triangle. The first character attached to an accelerometer indicates sensor location and the second character means sensor sensitivity in the figure; N stands for north, E for east, C for center, W for west, and U for upward. Servo accelerometer LS10C was used with an amplifier LF20 and 16-bit data recorder DA40, all of which are made by RION. The data acquisition system is applicable to 100 Hz with a sensitivity of about 3Gal for 16 bits. Observation duration was 10 minutes, of which a set of 10.24 sec stationary samples were collected for the analysis. Accelerometers at the center were used to compute H/V spectrum and four vertical accelerometers were used for Rayleigh wave dispersion curves.

Rayleigh wave phase velocities and H/V spectra are computed by BIDO 2.0 [2], which is distributed publicly on the web. CCA method [3] is adapted for phase velocity computation which is said to have an advantage over ordinary SPAC method in terms of longer wavelength, sometimes reaching to several tens of times of array radius. We exploit this advantage and use an array with a small radius of 0.9 m [4].

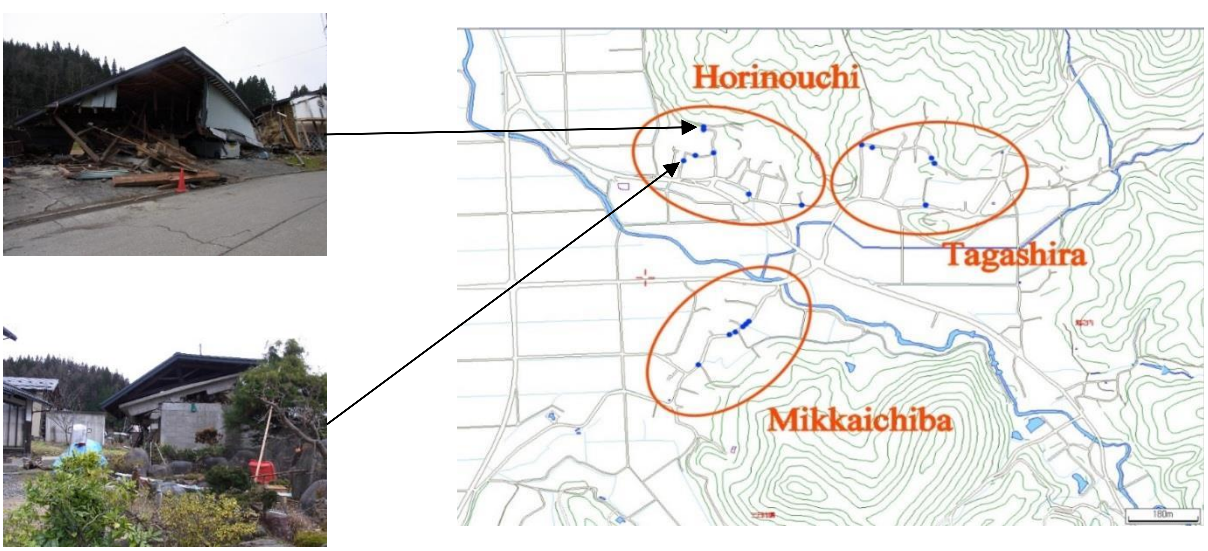

Fig. 1 – Location and photos of damaged houses in Kamishiro area

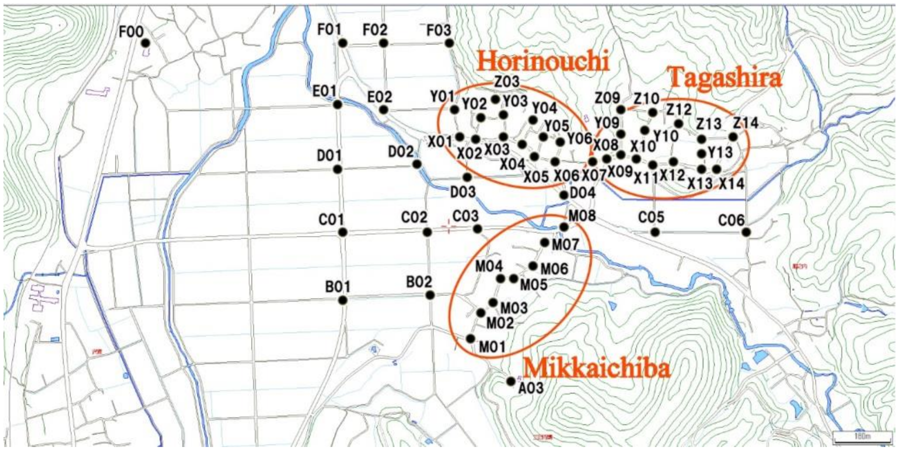

Fig. 2 – Observation points in the damage concentrated Kamishiro area

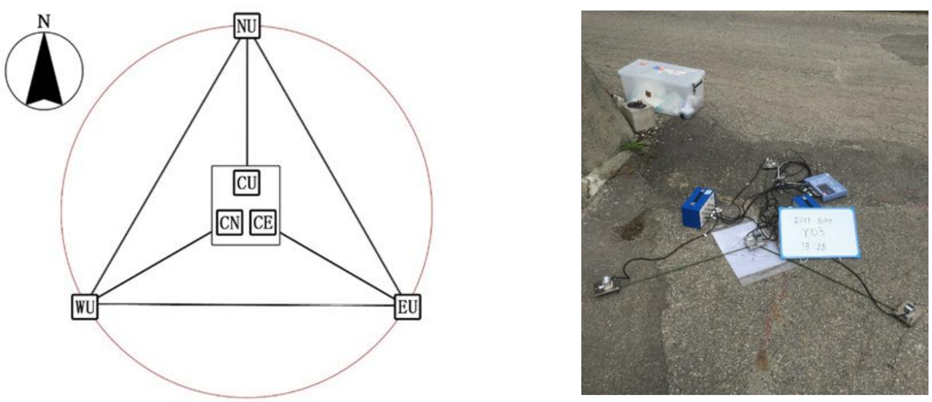

Fig. 3 – Array configuration and sensor arrangements

3. Phase velocity distribution by wavelength

Rayleigh wave phase velocity has been used for the evaluation of averaged S wave velocity [5]. We study dispersion curves by wavelength to directly relate phase velocity to subsurface layer thickness, though the ordinary expression of dispersion curves uses frequency for abscissa. Fig. 4 shows example dispersion curves in Horinouchi. We select 10m, 15m, 20m, and 25m for reference wavelengths and show the characteristics of the distribution of phase velocity.

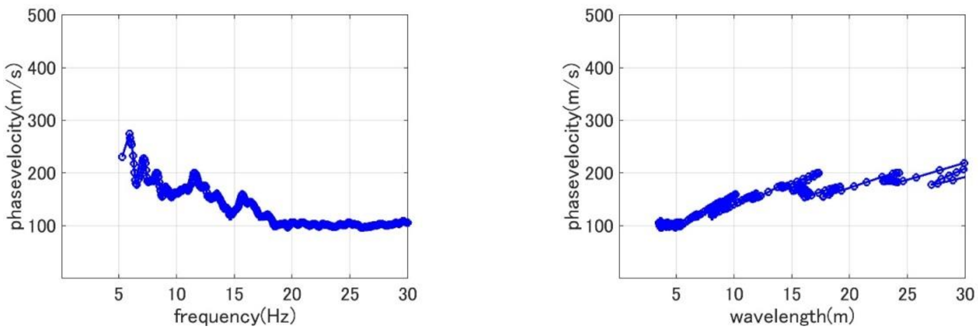

(a) Phase velocity by frequency

(b) Phase velocity by wavelength

Fig. 4 –Example dispersion curves at X07 in Horinouchi

3.1 Two dimensional distribution of phase velocity

Phase velocity contour diagrams with reference wavelength±0.5 m are shown for the Kamishiro area in Fig. 5. Points that lack phase velocity are marked in black. Those figures with different wavelength imply averaged surface layer shear wave velocity with different depth. Table 1 shows number of evaluated phase velocities. Decrease of the number with wavelengths implies difficulty in evaluation of velocity at longer wavelength.

Table 1 – Number of evaluated phase velocity by wavelength

wavelength	**10 m**	**15 m**	**20 m**	**25 m**
Within the allowance	55	52	49	46
Out of the allowance	0	3	6	9
total	55	55	55	55

From Fig. 5, larger Rayleigh wave phase velocity seems prevailing in longer wavelength in general, which implies normal sedimentation, i.e. stiffer soil at deeper layers. Phase velocity at D1, C1, and B1 in rice fields are similar with each other. They are lower than that in Horinouchi, Mikkaichiba, and Tagashira. Phase velocity at wavelength 20 m and 25 m is missing at A03, M01, and M02 in Mikkaichiba, which might mislead to different impression in the Fig. 5c and Fig. 5d.

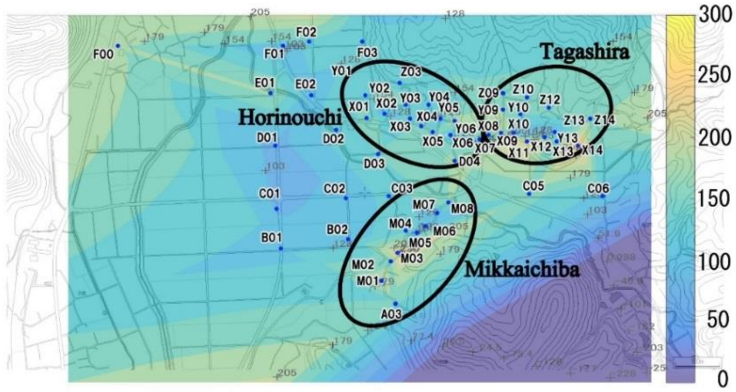

(a) 10 m

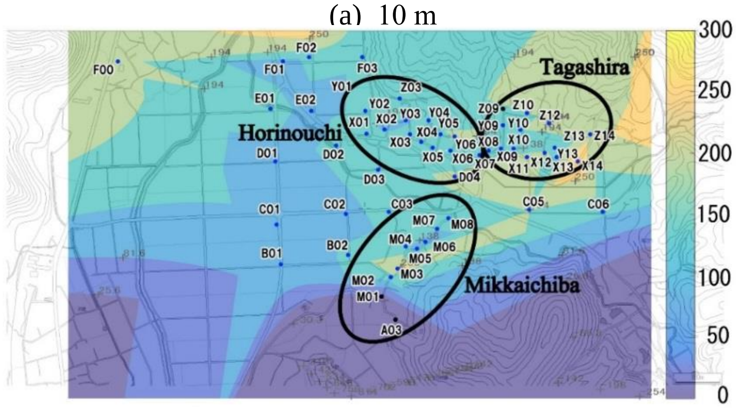

(b) 15 m

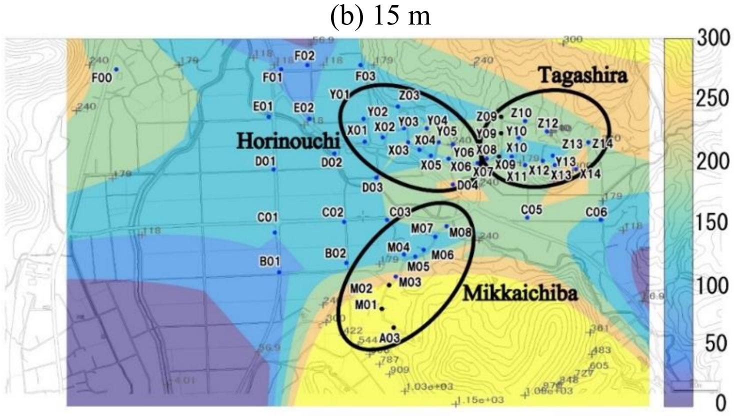

(c) 20 m

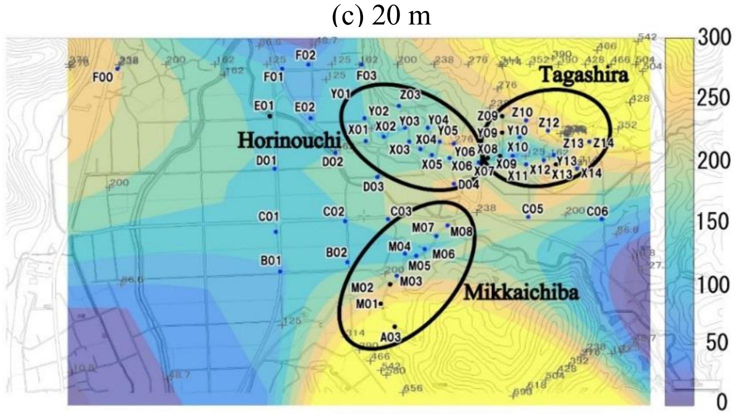

(d) 25 m

Fig. 5 – Distribution of phase velocity at different wave length

Fig. 6 shows detailed contour diagrams in Horinouchi. Color distribution is complex for the wavelength of 10 m and 25 m and the subsurface structure could be quite different even between neighboring points. Phase velocity for 15 m is mostly smaller than for 10 m implying the existence of weak layer at depth. Comparatively lower phase velocity is seen around Y03 and X02 especially at 15 m and 25 m. These two points are in the severest damage zone and subsurface layer with this low velocity may be attributable to the variability in damage. Y05 and Y06, the points on the east side near the mountain, have much larger phase velocity regardless of wavelength, and Y01at the west side shows invariant dark color at every wavelength implying thick soft soil layer. Fig. 7 shows detailed contour diagrams in Mikkaichiba. Phase velocities at 20 m and 25 m are not obtained in the southern part at A03, M01, and M02. Phase velocity decreases toward north to M05 and M06, then increases again to M08 toward the river.

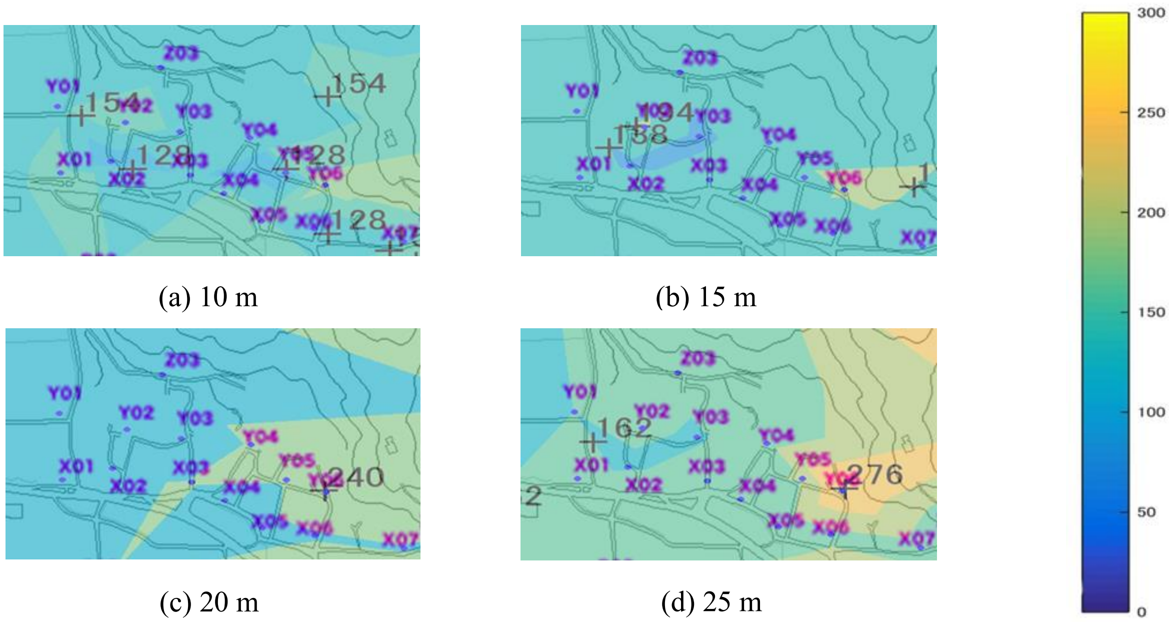

(a) 10 m (b) 15 m

(c) 20 m (d) 25 m

Fig. 6 – Distribution of phase velocity at different wave length in Horinouchi

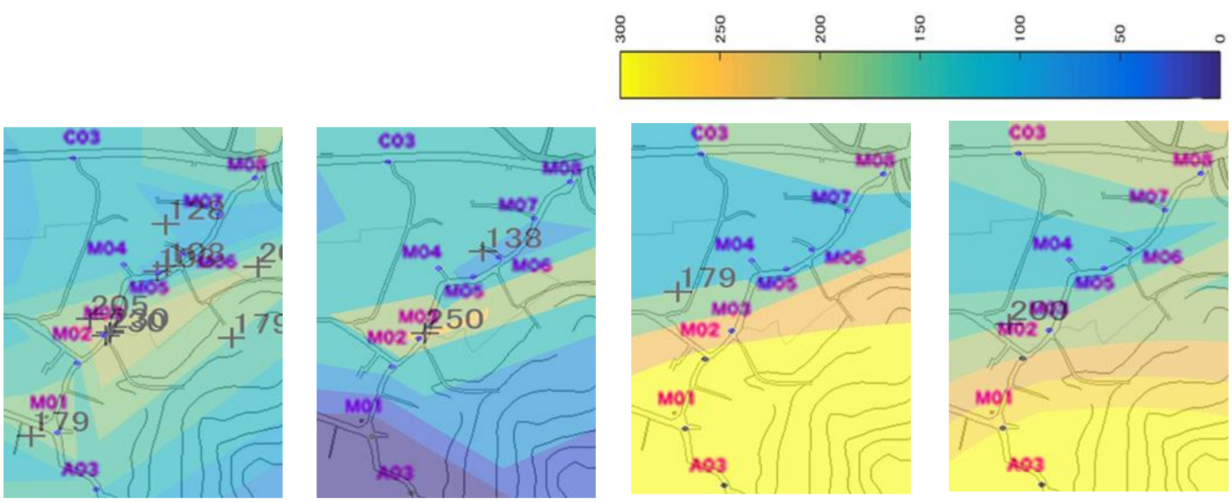

(a) 10 m (b) 15 m (c) 20 m (d) 25 m

Fig. 7 – Distribution of phase velocity at different wave length in Mikkaichiba

3.2. Phase velocity distribution along the measurement line

Phase velocity distribution along X line traversing Horinouchi and Tagashira is shown in Fig. 8a from east at X01 to west at X14. The velocity basically increases from east to west at every wavelength but has almost minimum velocity at X10 near the mountain foot regardless of wavelength. It stays almost constant at X04 and X05 implying a thick layer of single velocity. The distribution along Y line shown in Fig. 8b from east at Y01 to west at Y13 has similar tendency as X line but it is parted by the mountain at Y06. At Y05 and Y06, variation of velocity with wavelength is large, that implies rapid change of S wave velocity into depth. The distribution along M line from south to north is shown in Fig. 8c and Fig. 8d connecting to different line of 9th and 10th in Tagashira, respectively. Along M line in Mikkaichiba from south, the velocity decreases and then increases toward the river with minimum at M05 and M06 parting Horinouchi and Tagashira from Mikkaichiba. Along 9th line at the mountain side, the velocity does not change much, though the velocity along 10th line has a minimum at X10 coinciding the area minimum shown in Fig. 5.

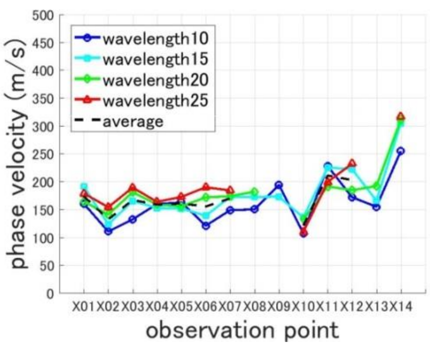

(a) X line

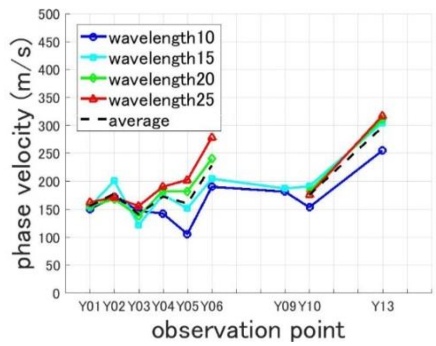

(b) Y line

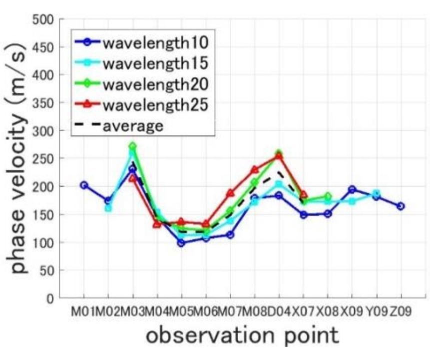

(c) M line and 9th line

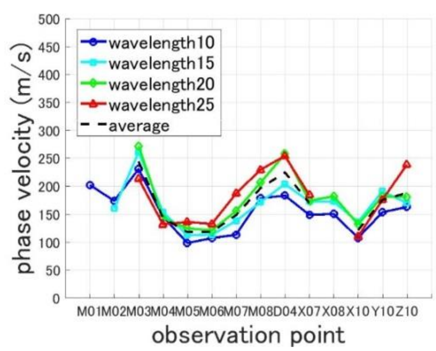

(d) M line and 10th line

Fig. 8 – Distribution of phase velocity along measurement lines

4. Distribution of surface layer thickness

4.1 S wave velocity of a surface layer

Shear wave velocity of a surface layer can be evaluated by Rayleigh wave phase velocity at a reference wavelength, which is proposed for the averaged shear wave velocity up to the depth of 30 m [5]. In this study, the reference wavelength is evaluated for the subsurface structure of K-NET Hakuba where the PS logging data is obtained as shown in Table 2. The theoretical dispersion curve based on the PS logging data deviates from the observed one as shown in Fig. 9a. We have tried to simulate the observed dispersion curve by increasing shear wave velocity uniformly at every layer in Table 2. The dispersion curve based on the revised model in Table 2 compares well with the observed one as shown in Fig. 9b.

Table 2– PS logging data and revised velocity structure for K-NET Hakuba

Layer No.	**Depth (m)**	**Thickness (m)**	**Mass Density (t/m^3)**	**Vs (m/s)**		**Averaged Vs (m/s)**		**1/4 wavelength freq. (Hz)**		**Vp (m/s)**	
				PS logging	Revised structure	PS logging	Revised structure	PS logging	Revised structure	PS logging	Revised structure
1	3	3	2.22	255	355	255	355	21.25	29.58	615	715
2	7	4	2.28	295	395	278	378	9.92	13.49	615	715
3	11	4	2.24	500	600	359	459	8.15	10.42	965	1065
4	20	9	2.23	850	950	580	680	7.25	8.50	1980	2080

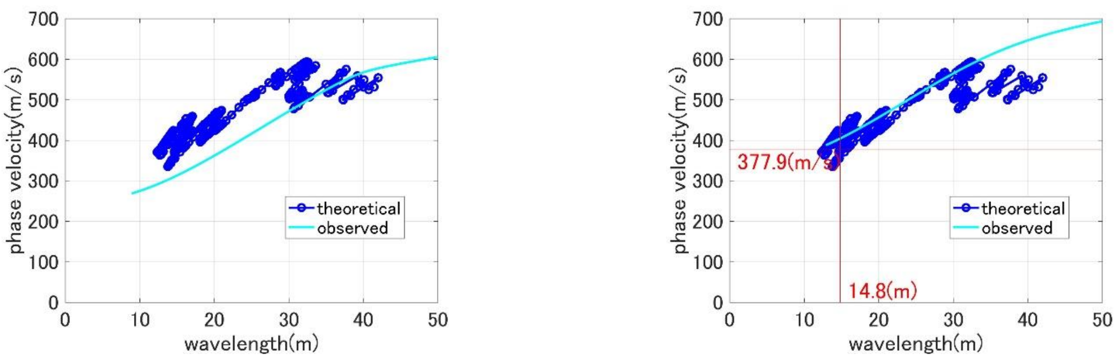

(a) PS logging data model

(b) Revised structure model

Fig. 9 – Comparison of the theoretical dispersion curves and the observed one

The reference wavelength is the wavelength at which the averaged surface layer velocity equals to Rayleigh wave phase velocity shown in Fig. 9b. In Table 2, the averaged surface layer shear wave velocity is 377.9 m/s up to 7 m where large velocity contrast exists, and the corresponding wavelength to this velocity is 14.8 m or rounded value of 15 m. In Kamishiro area, we hereafter quote surface layer shear wave velocity for Rayleigh wave velocity at the reference wavelength of 15 m. The distribution of the surface layer shear wave velocity is shown in Fig. 10. The velocity is high at the east part of Tagashira and in the middle of Mikkaichiba and relatively high between Mikkaichiba and Horinouchi as well as between Mikkaichiba and Tagashira. These high velocity parts partially encircle low velocity areas where the points X02, Y03, X04 in Horinouchi, X10, Y10 in Tagashira, and M04, M07, M08 in Mikkaichiba reside.

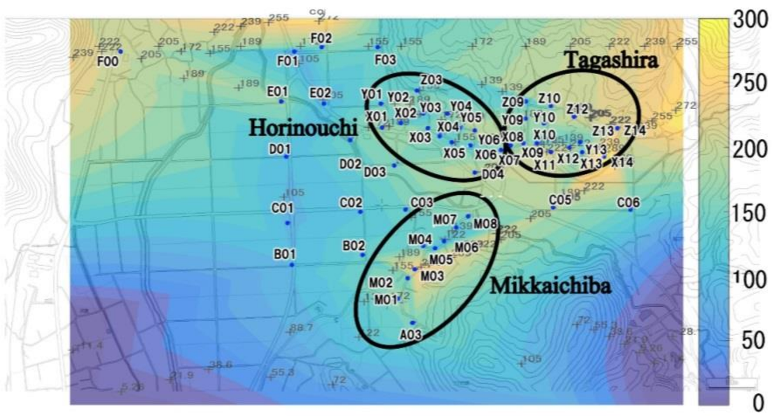

Fig. 10 – Distribution of surface layer S wave velocity deduced from Rayleigh wave velocity at the reference wavelength

4.2 Surface layer thickness

H/V spectrum is obtained by a square root of power spectrum ratio of horizontal component to vertical component, where the horizontal component is an average of EW and NS components. One of peak frequencies may represent predominant frequency of one part of the subsurface structure. Given the surface layer shear wave velocity *Vs* for the representative surface layer as in 4.1, corresponding layer thickness *H* can be evaluated from the predominant frequency *f* by the law of quarter wavelength as shown in Eq. (1).

$$H = \frac{Vs}{4f} \tag{1}$$

From Table 2, the law of quarter wavelength evaluates 13.5 Hz of the predominant frequency for the surface layer of 7 m with averaged Vs of 378 m/s. The observed H/V spectrum in Fig. 11 shows peaks around 4 Hz, 15 Hz, 17 Hz and more than 20 Hz. The estimated predominant frequency of 13.5 Hz corresponds to the one around 15 Hz, though we still have ambiguity in selecting the peak among peaks. The quoted surface layer shear wave velocity and one of the peak frequencies of H/V spectrum such as shown in Fig. 12 yields the distribution of surface layer thickness in Fig. 13. Surface layer thickness increases toward west in Horinouchi and moderately thick at the west of Tagashira across the mountain foot in between. Surface layer is relatively thick in the middle in Mikkaichiba. Y02, Y03, X02, X03, X04, X05 in Horinouchi, and M03, M04, M05, M06 in Mikkaichiba, where serious damage was observed, are located in the area of thick surface layer. Detailed distribution along the measurement lines shown in Fig. 14 also indicates that these points have thick surface layer. Though the points of serious damage in Tagashira, Z09, Z10, Z12, X12 are located in the area of relatively thin surface layer. It should be noted that the houses in Tagashira are located only along the road at the hillside.

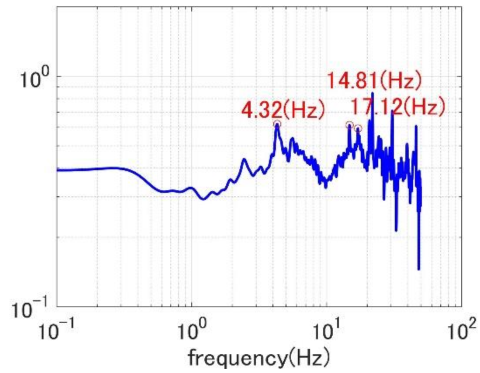

Fig. 11 –H/V spectrum at K-NET Hakuba

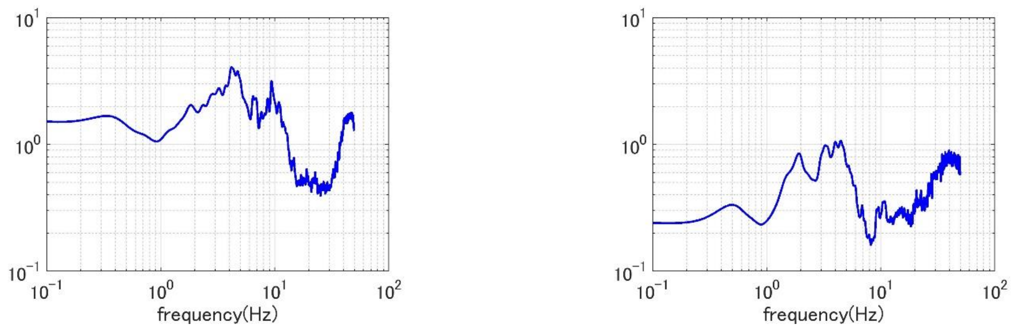

(a) X07 in Horinouchi

(b) C02

Fig. 12 – Example H/V spectra

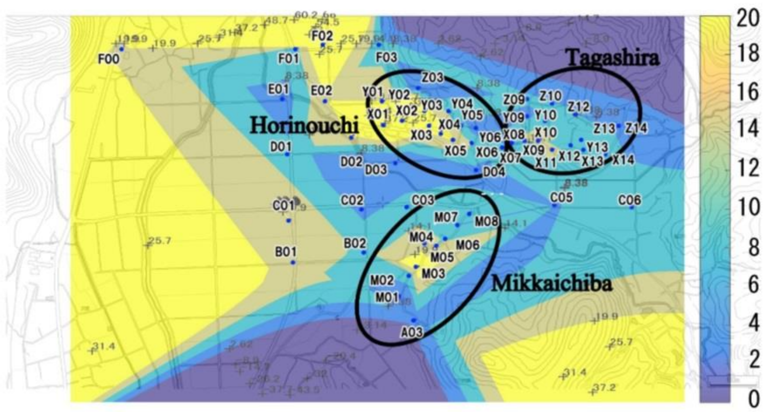

Fig. 13 – Distribution of surface layer thickness

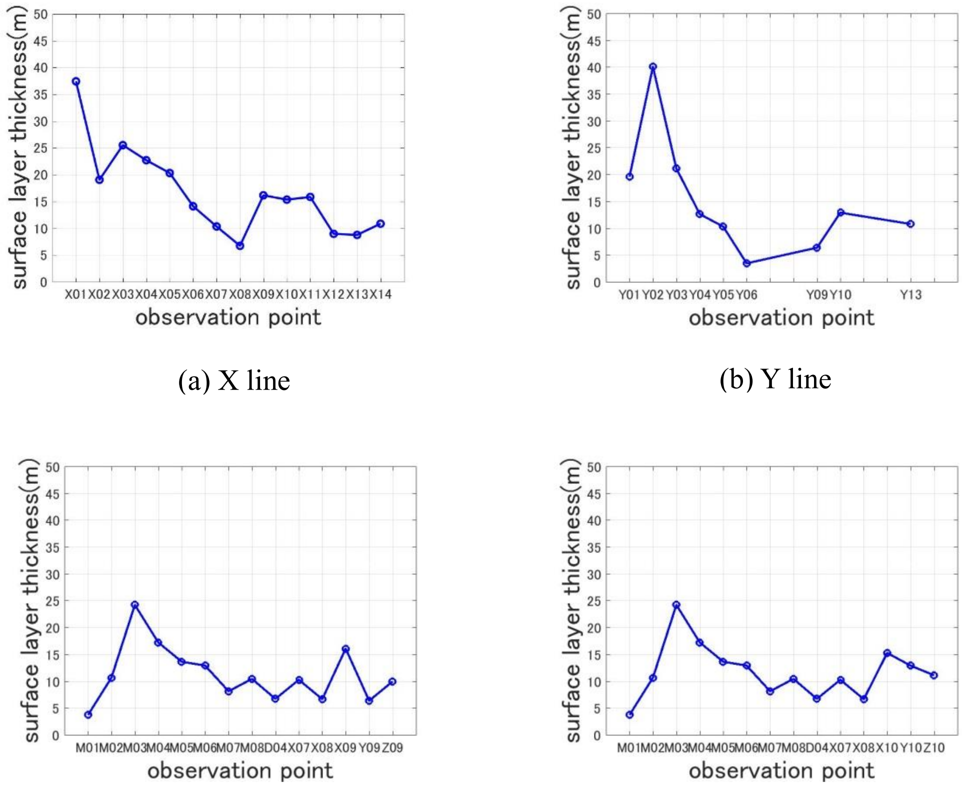

(a) X line

(b) Y line

(c) M line and 9th line

(d) M line and 10th line

Fig.14 – Distribution of surface layer thickness along measurement lines

5. Conclusion

At the 2014 Nagano prefecture Kamishiro fault Earthquake of magnitude 6.7, damaged houses were remarkably concentrated in two areas, namely Horinouchi and Mikkaichiba of Hakuba village. According to the former aftershock observation and micro-tremor array observation [1], soft layer can be partly attributable to the amplification of ground motion. But the amplification level is not high enough to explain the damage level and general conclusions have not been reached so far. We carried out micro-tremor miniature array observation at sixty points mainly in Horinouchi, Mikkaichiba, and Tagashira. Dispersion curves are studied by wavelength and the distribution of Rayleigh wave velocity at several wavelengths are analyzed. Rayleigh wave velocity is comparably low where the damage was concentrated.

K-NET Hakuba station is among the observation points. PS logging data at the station shows several subsurface layers. We take the one of the layer bottom as the bedrock and comparison of averaged shear wave velocity for layers above the bedrock and observed dispersion curve at the station gives us the idea of reference wavelength of 15 m. For all the observation points in the damage concentrated Kamishiro area, we adapted the reference wavelength and evaluated average surface layer shear wave velocity from the Rayleigh wave velocity. Surface layer thickness is evaluated by the law of quarter wavelength using the average surface layer shear wave velocity and one of the peak frequencies of H/V spectrum. Distribution of surface layer thickness reveals that the severely damaged area tend to have deep surface layer of low shear wave velocity encircled by high shear wave velocity zone.

The idea of the reference wavelength is inspired by the approximate method to evaluate the averaged shear wave velocity up to the depth of 30 m from Rayleigh wave dispersion curves. Though the reference wavelength should vary with the surface layer thickness from point to point, we used constant reference wavelength to show the concept of applying the idea to subsurface structure modeling. At the K-NET station, a subsurface model is revised from the one based on the PS logging data to comply with the observed dispersion curves. With the revised model, the predominant frequency evaluated by the quarter wavelength method corresponds to the one among several peaks of the observed H/V spectrum; though we still have ambiguity in selecting the peak among peaks. This ambiguity comes partly from the limited depth of the PS logging, and partly from the limited wavelength evaluated by small array radius.

6. Acknowledgement

We acknowledge to the members of Maeda Laboratory, department of Architecture, Waseda University, for their cooperation during the micro-tremor observation. We downloaded the analysis program BIDO 2.0 developed by Dr. Cho of National Institute of Advanced Industrial Science and Technology, Japan (http://www.cuee.titech.ac.jp/Japanese/Publications/Doc/conference_7th.pdf). Discussion with Dr. Cho and Dr. Yasui, an adjunct researcher at Research Institute for Science and Engineering, Waseda University greatly helped deepening our understanding on CCA method. This work was partly supported by Waseda University Grant for Special Research Projects (2015B-226).

7. References

[1] Chimoto K, Yamanaka H, Saguchi K, Tsuno Y, Iiyama K (2016): Evaluation of site amplification in Hakuba from observations of microtremors and aftershocks of the 2014 Northern Nagano Earthquake, *J. Struct. Eng., AIJ*, **8** (719), 51-59 *(in Japanese).*

[2] Tada T, Cho I, Shinozaki Y (2010): New Horizons in the utility of horizontal-motion microtremors. *Proc.7th International Conference on Urban Earthquake Engineering, Center for Urban Earthquake Engineering, Tokyo Institute of Technology*.

[3] Cho I, Tada T, Shinozaki Y (2006): Centerless circular array method: Inferring phase velocities of Rayleigh waves in broad wavelength ranges using microtremor records, *JGR*, 111, B09315.

[4] Cho I, Senna S, Fujiwara H (2013): Miniature array analysis of microtremors, *GEOPHYSICS,* **78** (1), KS13–KS23.

[5] Konno K, Kataoka S (2000): An Estimating method for the average S- wave velocity of ground from the Phase velocity of Rayleigh wave, *Proceedings of JSCE* 647, 415-423.